Membrane heterogeneity : from lipid domains to curvature effects

Semrau, S.

Chapter 6

Role of membrane heterogeneity and precoupling in Adenosine A_1 receptor signaling unraveled by Particle Image Correlation Spectroscopy (PICS)

We use the recently developed particle image correlation spectroscopy (PICS) to unravel the influence of spatial membrane organization on adenosine A_1 *receptor signaling. It turns out that the diffusion behavior of the receptor can be used as a faithful readout of its activation state. We identify slowed diffusion with localization of the receptor in membrane microdomains. Stimulation experiments show that 9 % of the receptors translocate to* $\approx$ *130 nm sized domains upon agonist exposure. In experiments on cell blebs this structure is lost. This shows that the observed domains are closely linked with the cytoskeleton. Decoupling of receptor and G protein leads to an increase in receptor mobility in 7 % of the cases. This we take as evidence for receptor G-protein precoupling corroborating that the G protein is responsible for the interaction with microdomains.*

6.1 Introduction

The adenosine A_1 receptor is involved in many physiological processes ranging from neuroprotective mechanisms in the brain (197) to the control of heart rate (144). It belongs to the superfamily of G-protein coupled receptors (GPCRs), of which many fulfill clinically significant functions. For this reason, and because many GPCRs are conveniently localized in the cell's plasma membrane, they are attractive drug targets (144). The wish to create more effective and specific drugs motivates the interest in understanding GPCR signaling. Since the first steps of GPCR signaling take place in the membrane, membrane organization is closely linked to signaling and is therefore eventually important for drug design. A recent study could indeed show that targeting a drug to the membrane can improve its efficacy (198).

While the overall mechanism of GPCR signaling is well understood, the putative role of membrane organization remains unknown. In the canonical model for GPCR signaling, the signaling cascade is initiated by the binding of an agonist, see Fig. 6.1 a. Upon binding the receptor undergoes a conformational change (it becomes active),Fig. 6.1 b, and gains the ability to interact with its G protein, Fig. 6.1 c. The G protein is then in turn activated and the cascade processes downstream, Fig. 6.1 d. The interaction between G protein and receptor is known to happen on the same time scale as the conformational change of the receptor (145). In other words, the receptor G protein interaction happens very quickly, almost instantaneously, after ligand binding (146). That suggest that G protein and receptor are precoupled. However, experimental attempts to verify this give contradictory results (145, 147, 148). The existence of precoupling is therefore still actively discussed (199). Alternatively, receptor and G protein could be co-localized in small membrane domains. This would also significantly reduce the time necessary to interact. Such signaling platforms could furthermore play a role in receptor desensitization and internalization (13).

In recent years several mechanisms for the formation of membrane domains have been discussed. In addition to structures like caveolae and clathrin coated pits, lipid phase separation (lipid rafts)(9, 10, 18, 19, 157, 200) and the underlying actin cortex (picket fence model) (29, 35) were hypothesized to give rise to microscopic structure.

Since this structure influences the diffusion behavior of membrane proteins, receptor movement is an excellent readout for the involvement of

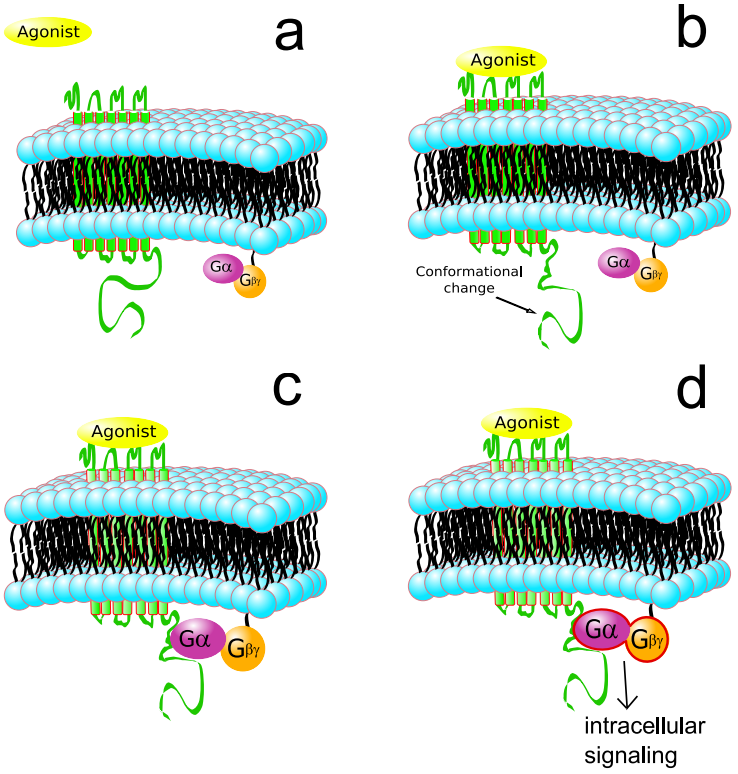

Figure 6.1
Model for GPCR signaling

membrane organization during signaling. The typical size of membrane domains requires methods that can assess molecular motion on a nanometer length scale and a millisecond time scale. These requirements make single molecule experiments the method of choice (98), optical probes used to tag the protein of interest can be localized with down to a few nanometer precision at a temporal resolution of a few milliseconds (see (111) (Chap. 5 of this thesis) and references therein).

For the measurement of receptor motion, fluorescent proteins turn out to be suitable optical tags. They can be fused to the receptor and guarantee therefore a one-to-one labeling ratio. In contrast to most other probes they can be attached to the cytosolic part of the receptor which reduces interference with ligand binding. Fluorescent proteins are also small com-

pared to other conventional probes like gold beads, labeled antibodies or quantum dots. However, the complex photophysics of these proteins (109) was long considered a serious hurdle for their use. Indeed, blinking and bleaching render the construction of single molecule trajectories difficult. In order to overcome these problems, we developed particle image correlation spectroscopy (PICS). In contrast to conventional particle tracking methods, PICS allows the robust determination of mean squared displacements (MSDs) and eventually diffusion coefficients without any a priori knowledge about diffusion speeds. In fact, the photophysics of fluorescent proteins can even be exploited in the following way. Fluorescent proteins can enter long lived dark states or a reversible bleached state which show no fluorescence. However, they recover to a fluorescent state on time scales from milliseconds to seconds (109) . In conventional tracking this is considered problematic because the molecule cannot be followed while it is dark. The reconstruction of a trajectory is therefore very difficult. Since PICS does not require uninterrupted trajectories, long lived dark states or reversible bleached states actually extend the period of time over which the receptor diffusion can be accessed.

Here we present the application of PICS to the signaling of the adenosine A_1 receptor. With the help of stimulation experiments on living cells we address the role of membrane heterogeneity in the signaling process. We compare the results in living cells to the receptor movement in cell blebs to find out if the cytoskeleton is responsible for some of the observed effects. We furthermore observe the change in diffusion behavior after decoupling of receptor and G protein to answer the question whether there is receptor G-protein precoupling.

6.2 Materials and Methods

6.2.1 Single-molecule microscopy

The experimental setup for single-molecule imaging has been described in detail previously (131). Briefly, the microscope (Axiovert 100; Zeiss, Oberkochen Germany) was equipped with a 100x oil-immersion objective (NA=1.4,Zeiss, Oberkochen, Germany). The samples were illuminated for 3 ms by an Ar^+ laser (Spectra Physics, Mountain View, CA, USA) at wavelength of 514nm. The illumination intensity was set to $2 \pm 0.2\,\mathrm{kW/cm^2}$. Use of an appropriate filter combination (DCLP530, ET550/50m or HQ570/80, Chroma Technology, Brattleboro,USA) per-

mitted the detection of individual fluorophores by a liquid nitrogen cooled slow-scan CCD camera system (Princeton Instruments, Trenton, NY, USA). The total detection efficiency of the experimental setup was $\eta = 0.12$. For the experiments the camera was run in the kinetics-mode, permitting the recording of 8-10 images in sequence before reading out. The time between consecutive images (time lag) was set to 5-50 ms. 25-100 sequences (of 8-10 images) per cell were obtained for each time lag.

For the observation of the mobility of individual eYFP-A_1 molecules, CHO cells adhered to glass slides were mounted onto the microscope and kept in phosphate buffered saline (DPBS + $CaCl_2$ + $MgCl_2$, Gibco Invitrogen, Carlsbad, USA) at $37.5°C$ for the experiments on decoupling the G-protein from the receptor and $26°C$ for the agonist stimulation experiments (see below). In the case of the decoupling experiments pertussis toxin from *Bordetella pertussis* (PTX) was added to a final concentration of 100 ng/ml (see below). In the agonist stimulation experiments 2-chloro-N^6-cyclo-pentyladenosine (CCPA) was added to a final concentration of 400nM (see below)

The focus of the microscope was set to the dorsal surface membrane of individual cells (depth of focus $\approx 1\mu m$). The density of fluorescent proteins on the plasma membrane of selected transfected cells was below $1\mu m^{-2}$ to permit imaging of individual fluorophores. Molecule positions were determined with an accuracy of $\approx 42\,nm$.

6.2.2 Particle Image Correlation Spectroscopy (PICS)

The reconstruction of trajectories from molecule positions is severely hampered by the blinking and photobleaching of eYFP (110). Therefore we use an alternative analysis method, Particle Image Correlation Spectroscopy (PICS), described in detail elsewhere (111) (Chap. 5 of this thesis). In short, the cross-correlation between single-molecule positions at two different times is calculated. Subsequently, the linear contribution from uncorrelated molecules in close proximity is subtracted. This results in the cumulative distribution function $P(l, \Delta t)$ for the length l of diffusion steps during the time lag Δt. For each time lag P is fitted to a two fraction

model

$$P(l,\Delta t) = \alpha\left(1-\exp\left(-\frac{l^2}{sd_1(\Delta t)}\right)\right) + (1-\alpha)\left(1-\exp\left(-\frac{l^2}{sd_2(\Delta t)}\right)\right) \tag{6.1}$$

where the free parameters are $sd_1(\Delta t)$ and $sd_2(\Delta t)$, the square displacements of the two fractions, and the fraction size α. We choose α to be the size of the faster fraction. A mean value of the fraction size α is determined from the results for longer time lags (50 - 250 ms) where the fit is most trustworthy. The data is then refitted with α fixed to the mean value just established. This decreases the number of free parameters to 2 ($sd_1(\Delta t)$ and $sd_2(\Delta t)$) and therefore improves the quality of the fit.

6.2.3 Analysis of MSDs (Mean square displacements)

The mean square displacements of the two fractions $sd_1(\Delta t)$ and $sd_2(\Delta t)$ are subsequently fitted to a walking diffusion model (133), see Fig. 6.3. In this model a random walker diffuses quickly with D_{micro} within a domain of size L which in turn moves slowly with D_{macro}. The model is fully equivalent to hopping diffusion where the pickets of a protein fence hinder diffusion on a macroscopic scale. The MSD is given by

$$sd(\Delta t) = \frac{L^2}{3}\left[1-\exp\left(-\frac{12D_{\text{micro}}\Delta t}{L^2}\right)\right] + 4D_{\text{macro}}\Delta t \tag{6.2}$$

Fit parameters are the microscopic and macroscopic diffusion coefficients D_{micro} and D_{macro} and the domain size L. This model gives a very good description of the data.

6.2.4 Cell culture

For all experiments a Chinese Hamster Ovary (CHO) cell line (clone D3) stably expressing the human adenosine A_1 YFP receptor construct (201, 202) was used. Cells were cultured in DMEM:F12 1:1 medium supplemented with streptomycin (100 μg/ml), penicillin (100 U/ml) and 10% new born calf serum in a 7% CO_2 humidified atmosphere at 37°C. Cells were used for 25-30 passages and were transferred every 4 days.

For microscopy cells were cultured on cover glass slides (Assistent, Karl Hecht KG, Sondheim, Germany). For most experiments healthy looking cells were used (see Fig. 6.2,left). For comparison, some measurements were taken on cell blebs, expelled from untreated, apoptotic cells (see Fig. 6.2,right).

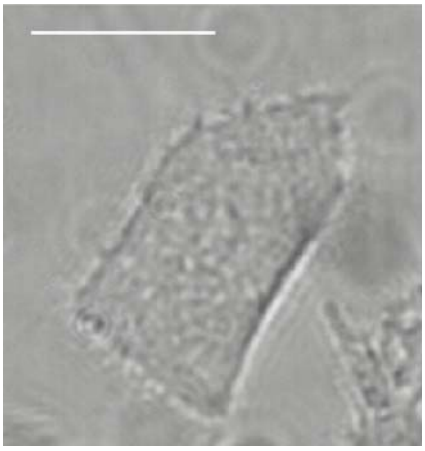

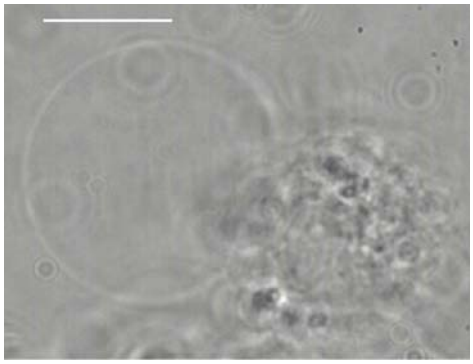

Figure 6.2
Left: untreated CHO cell, Right: cell bleb expelled from an apoptotic CHO cell, scale-bar: 10 μm

6.2.5 Agonist stimulation assay

The activation of the adenosine A_1 receptor was achieved by the addition of 2-chloro-N^6-cyclo-pentyladenosine (CCPA) to a final concentration of 400nM. CCPA is known to be a potent agonist of the adenosine A_1 receptor (197, 201). Since the binding affinity of CCPA is $6.4nM$ (197), all receptors should be activated at the CCPA concentration used. The receptor mobility was measured before stimulation and after 20 minutes of continuous stimulation.

6.2.6 Decoupling of G-protein with Pertussis toxin

Cells were incubated for 16h (basically overnight) and during observation with 100 ng/ml pertussis toxin from *Bordetella pertussis* (PTX) (Sigma-Aldrich,) Pertussis toxin is known to decouple the GPCR from its G-protein by catalysing the ADP-ribosylation of the G-protein α subunit(203).

6.3 Results

We performed single molecule microscopy experiments on the adenosine A_1 receptor in living CHO cells. For each experimental situation we determined the mean squared displacement(MSD) of the receptor with respect to time by particle image correlation spectroscopy (PICS).

Throughout all experiments the MSD is clearly non-linear, see e.g. Fig. 6.5, which reflects the heterogeneity of the membrane. On small length scales (D_{micro}) diffusion is considerably faster than on longer length scales (D_{macro}). Therefore, we use a walking diffusion model to describe the data, see Fig. 6.3. By fitting of Eq. 6.2 we determine D_{micro} and D_{macro} and the domain size L. The results for all experimental situations are summarized in Table 6.1.

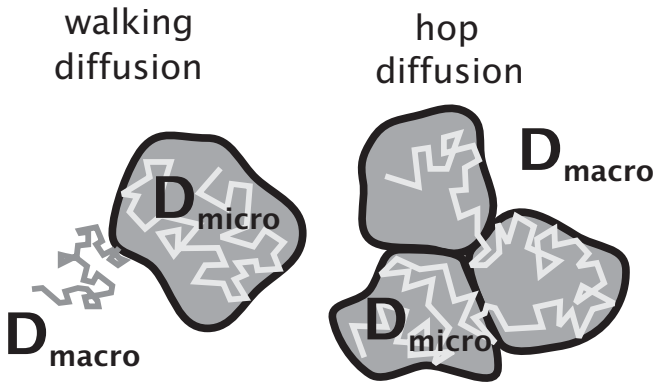

Figure 6.3
Walking diffusion (left) and hopping diffusion (right) both give rise to different diffusion coefficients on different length scales.

In addition to the non-linearity of the MSDs we find that the diffusion behavior of the receptor cannot be described by a single MSD. Throughout all experiments on living cells we find two receptor fractions with different diffusion behaviors. As can be seen from Table 6.1, microscopic and macroscopic diffusion coefficients differ at least by a factor of 3. Therefore the two fractions are dubbed "slow" and "fast" respectively. We find the size of the fast fraction to be on average 73%±2%. We find $D_{\text{fast}}0.47\pm0.12$ and $D_{\text{slow}}0.1 \pm 0.02$ at $37.5°C$ and $D_{\text{fast}}0.15 \pm 0.28$ and $D_{\text{slow}}0.05 \pm 0.03$ at $26°C$.

6.3.1 The activated receptor translocates to microdomains

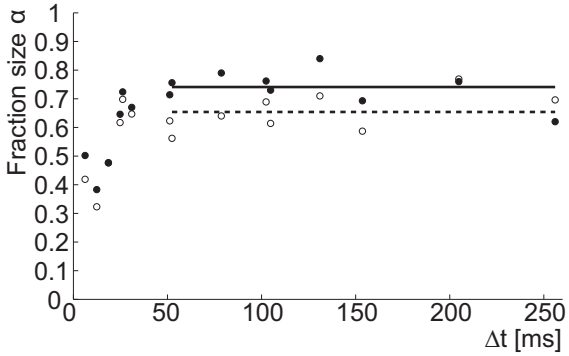

Figure 6.4
Relative size of the fast fraction (α) for the control (solid circles) and after 20 minutes of agonist stimulation (open circles). Average of the interval 50 - 256 ms gives $\alpha = 0.74 \pm 0.02$ for the control (solid line) and $\alpha = 0.65 \pm 0.02$ after stimulation (dashed line)

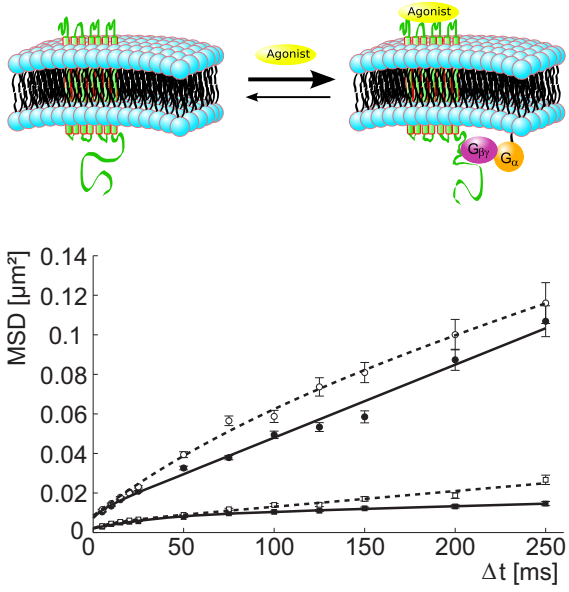

Figure 6.5
Mean square displacements of the control (solid circles: fast fraction, solid squares: slow fraction) and after 20 minutes of agonist stimulation (open circles: fast fraction, open squares: slow fraction). The lines are fits of a walking diffusion model (Eq. (6.2)) (solid lines: control, dashed lines: after stimulation. The results of the fits are given in Table 6.1).

In order to identify the two different fractions we stimulate the receptor with the agonist CCPA. Stimulation shifts the equilibrium to the activated receptor. We find that agonist stimulation decreases the size of the fast fraction α from $74\% \pm 2\%$ to $65\% \pm 2\%$,see Fig. 6.4, while the microscopic and macroscopic diffusion coefficients stay approximately the same, see Fig. 6.5 and Table 6.1. Consequently, the activated receptor must be part

of the slow fraction. The change in conformation of the receptor or the size difference between the plain receptor and the receptor-G protein complex cannot explain the difference in diffusion speed between the fast and the slow fraction (204, 205). Therefore, the receptor-G protein complex must be either localized in membrane microdomains with a higher membrane viscosity or associated with the cytoskeleton. Especially in the latter case the G-protein, which protrudes into the cytosol, might be responsible for the slow speed of the activated receptor. In our measurements we can retrieve the domain size from the walking diffusion model and we find a domain size of about 130 nm for the slow fraction and 250 nm for the fast fraction.

6.3.2 The observed microdomains are related to the cytoskeleton

To determine the connection of the membrane microdomains to the cytoskeleton we repeated the control experiment (i.e. unstimulated) in cell blebs. In cell blebs, which appear during apoptosys, the cytoskeleton is detached from the membrane. It has been observed that the lateral diffusion speed of certain membrane receptors is increased (206), which was ascribed to the release of lateral constraints. In our experiments we find very similar effects, see Fig.6.6 and Table 6.1. The diffusion coefficient is increased by a factor of 6 compared to the fast fraction of the previous experiments and there is no slow fraction anymore. This means that for the domains observed in our experiments the cytoskeleton is essential.

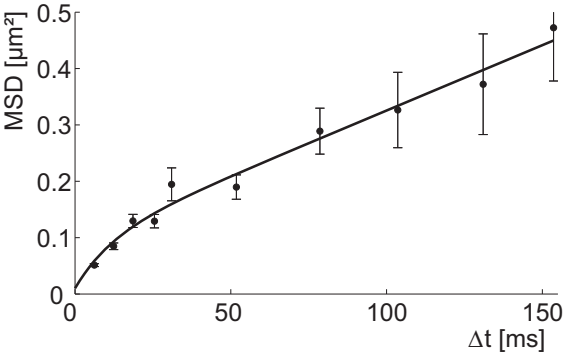

Figure 6.6
Mean square displacements of the receptor diffusion in a cell bleb (solid circles). The line is a fit of a walking diffusion model (Eq. (6.2)*) The result of the fit is given in Table 6.1).*

6.3.3 The receptor is partially precoupled to its G-protein

On top of the the localization in domains, G-protein and receptor could still be precoupled. Furthermore it is still unclear if coupling to the G-protein causes the slow receptor fraction to be slow. To address these questions we decouple putatively precoupled complexes by applying pertussis toxin (PTX).

Decoupling of the receptor from its G-protein causes the fast fraction α to grow, see Fig. 6.7, from 71%±2% to 78%±1%, while the other diffusion parameters do not change, see Fig. 6.8 and Table 6.1. This result is in agreement with the stimulation experiment in which the opposite effect was observed upon receptor stimulation. Consequently, at least 7% of the receptors is precoupled to the G-protein.

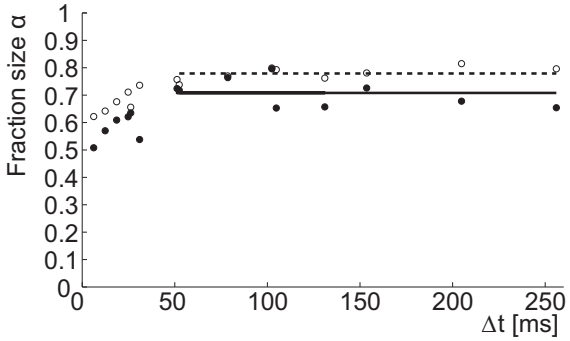

Figure 6.7
Relative size of the fast fraction (α) for the control (solid circles) and after PTX treatment (open circles). Average of the interval 50 - 256 ms gives $\alpha = 0.71 \pm 0.02$ for the control (solid line) and $\alpha = 0.78 \pm 0.01$ after PTX treatment (dashed line).

6.4 Discussion

In the present work we show that membrane heterogeneity influences adenosine A_1 receptor signaling. Consistently, we find highly non-linear MSDs and two receptor fractions which differ in diffusion coefficient. Two different diffusion coefficient were already found in earlier experiments by Briddon et al. (207) on an antagonist bound to the adenosine A_1 receptor ($D_{\text{fast}} = 0.43\mu m^2/s, D_{\text{slow}} = 0.05\mu m^2/s$). Since these results were obtained by FCS in small membrane areas, the values found are comparable to the microscopic diffusion coefficients found in our experiments, $D_{\text{fast}}0.47 \pm 0.12$ and $D_{\text{slow}}0.1 \pm 0.02$ at $37.5°C$ and $D_{\text{fast}}0.15 \pm 0.28$ and $D_{\text{slow}}0.05 \pm 0.03$ at $26°C$. Briddon et al. ascribed the slow fraction to antagonist molecules bound nonspecifically to the membrane. They ad-

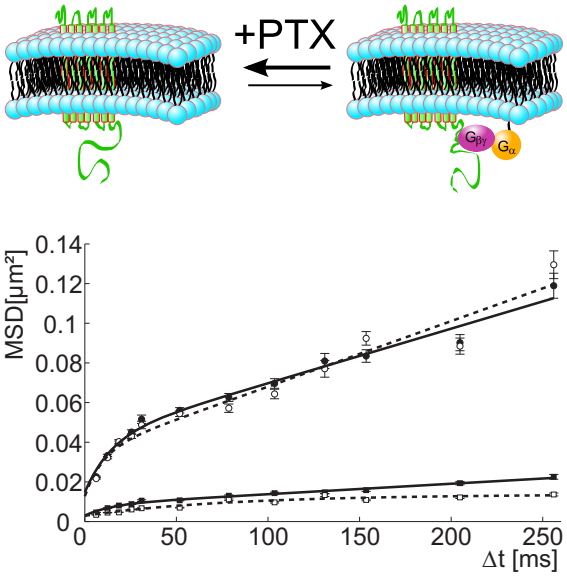

Figure 6.8
Mean square displacements of the control (solid circles: fast fraction, solid squares: slow fraction) and after PTX treatment (open circles: fast fraction, open squares: slow fraction). The lines are fits of walking diffusion model (Eq. (6.2)) (solid lines: control, dashed lines: after PTX treatment. The results of the fits are given in Table 6.1).

	fraction	α	D_{micro} $[\mu m^2/s]$	D_{macro} $[\mu m^2/s]$	L $[nm]$
control	fast	0.71 ± 0.02	0.47 ± 0.12	0.07 ± 0.01	287 ± 20
	slow		0.10 ± 0.02	0.01 ± 0.001	129 ± 7
PTX overnight	fast	0.78 ± 0.01	0.58 ± 0.35	0.08 ± 0.01	258 ± 31
	slow		0.03 ± 0.005	0.001 ± 0.006	173 ± 64
control	fast	0.74 ± 0.02	0.15 ± 0.28	0.09 ± 0.004	107 ± 35
	slow		0.05 ± 0.003	0.006 ± 0.0006	135 ± 5
20 min stimulation	fast	0.65 ± 0.02	0.10 ± 0.02	0.07 ± 0.02	337 ± 133
	slow		0.05 ± 0.03	0.02 ± 0.002	93 ± 17
Blebs			1.76 ± 0.91	0.58 ± 0.07	501 ± 86

Table 6.1
Overview of results. α size of fast fraction, D_{micro} microscopic diffusion coefficient, D_{macro} macroscopic diffusion coefficient, L domain size

mitted, however, that more rigid membrane domains could also be responsible for the slowed diffusion. Our results for the movement of the receptor show that this is indeed the case. The difference in diffusion speed between the fast and the slow fraction is too big to be explained by a change in conformation of the receptor or the size difference between the plain receptor and the receptor-G protein complex(204, 205). Consequently, membrane microdomains with a higher membrane viscosity or interaction

with the cytoskeleton must be responsible for the slowed diffusion. The conclusion is in qualitative agreement with results on the A_3 receptor in CHO cells (208). Cordeaux et al. found two different fractions where the slower fraction is identified with receptors partitioned in membrane microdomains. The size of those domains was not determined. In this work we obtain the domain sizes from the walking diffusion model and find 130 nm for the slow fraction and 250 nm for the fast fraction. These values are in agreement with scanning force microscopy experiments on living CHO cells by Lucius et al. (209). They find two populations of pits with mean diameters of around 100 nm and 200 nm. The smaller structures are speculated to be caveolae. With this interpretation our findings are consistent with earlier results by Escriche et al. (210). Their experiments show that the adenosine A_1 receptor translocates to caveolae after ligand binding. Correspondingly, we find that the slow receptor fraction increases after ligand binding by 9 percent points.

In our experiments on cell blebs, in which the actin cortex is detached from the membrane, membrane microstructure is no longer observable. This indicates that the cytoskeleton is essential for the observed heterogeneity. However, the cytoskeleton does not necessarily directly give rise to receptor confinement as assumed in the picket fence model (29). It might rather assist the assembly of heterogeneities like caveolae or clathrin coated pits and hinder the movement of those domains.

Furthermore, our experiments show that coupling of the receptor with its G protein plays an important role in the interaction with membrane heterogeneities. Upon decoupling of receptor and G protein, the fast receptor fraction increases by 7 percent points. From this, we can conclude that 1. There is precoupling between the receptor and its G protein and 2. The G protein is responsible for the interaction of the complex with membrane domains. In earlier experiments by Briddon et al. (207) faster diffusion was observed upon treatment with an antagonist. Given that an antagonist effectively causes decoupling of G-protein and receptor this result is consistent with our findings.

Comparison of our results to other GPCRs (211) show that signaling mechanisms vary, even within the same receptor class. Charalambous et al. (211) show that the mobility of the adenosine A_{2A} receptor is unaffected by agonist binding and they do not detect a significant amount of precoupling. They furthermore find that the adenosine A_{2A} receptor is localized in microdomains which are sensitive to cholesterol depletion.

These different influences of membrane organization on GPCR signaling might eventually lead to the development of highly specific drugs, which are targeted to the membrane (198).

The new insights obtained in this work were made possible by a novel technology: particle image correlation spectroscopy can be successfully used to elucidate the relevance of spatial membrane organization for signaling networks. It provides quantitative results about diffusion coefficients and confinement sizes which are vital parameters for models describing such networks.